Z. Phys. B - Condensed Matter 47, 285–291 (1982)

Condensed
Zeitschrift für Physik B Matter

Impact Ionization Induced Negative Far-Infrared Photoconductivity in *n*-GaAs

E. Schöll[a], W. Heisel[b], and W. Prettl[b]

[a] Institut für Theoretische Physik, Rheinisch-Westfälische Technische Hochschule Aachen, Federal Republic of Germany

[b] Institut für Angewandte Physik der Universität, Regensburg, Federal Republic of Germany

Received February 8, 1982

Far-infrared photoconductivity of *n*-GaAs epitaxial layers showing impact ionization breakdown has been investigated by molecular lasers at photon energies below the $1s-2p$ shallow donor transition energy. Negative photoconductivity was observed if a magnetic field was applied to the crystals and if impact ionization of donors by the electric bias field was the dominant electron excitation mechanism. The experimental results are qualitatively explained on the basis of the generation-recombination kinetics of electrons bound to donors. Negative photoconductivity is attributed to optically induced free to bound transitions of electrons from the $N=0$ Landau band to donor levels shifted by the magnetic field above the low energy edge of the conduction band.

I. Introduction

Impact ionization of shallow impurities has been observed in many semiconductors [1–4]. At low temperatures almost all carriers are bound to localized impurities or to very low mobility impurity bands. An electric field of the order of a few volts per cm provides sufficient energy to enable impact ionization of occupied impurities. This results in a strong increase of the current at a critical electric breakdown field depending on impurity concentration, compensation ratio, magnetic field and temperature. Impact ionization of shallow impurities may be accompanied by several interesting nonlinear phenomena like current controlled negative differential resistance [2, 5, 6], photoinduced switching [4], and photocurrent multiplication [7]. In a previous publication we reported on negative far-infrared photoconductivity i.e. a decrease in conductivity by irradiation which was observed in *n*-GaAs under impact ionization conditions if a magnetic field was applied to the sample [8]. In this paper we will discuss the characteristic behaviour of far-infrared photoconductivity of *n*-GaAs as a function of various parameters like the magnetic field, the electric bias field, the current and the laser power and we will present a model which explains the occurrence of negative photoconductivity and which describes the experimental results. The model is based on the nonlinear generation-recombination kinetics of electrons in the presence of shallow donors subjected to a magnetic field. The essential features of the model are optically induced transitions of free electrons from the lowest Landau level to energetically higher bound donor states. Such excitations reduce the conduction electron concentration and may produce negative photoconductivity if the $N=0$ Landau subband is highly populated by impact ionization of shallow donors.

II. Experimental

a) Technique

The experiments were carried out on *n*-GaAs epitaxial layers whose properties are given in Table 1. The samples mounted in a metallic light pipe were immersed in liquid helium at the center of a superconducting magnet. Cold crystalline quartz and black polyethylene filters were applied to eliminate visible light and to reduce the thermal background radiation. The photoconductivity was measured

0722-3277/82/0047/0285/$01.40

Table 1. Donor concentration N_D, acceptor concentration N_A, mobility μ at 77 K and thickness d of the investigated epitaxial layers. In all samples negative photoconductivity was observed

Samples	$N_D/10^{14}\,\mathrm{cm}^{-3}$	$N_A/10^{14}\,\mathrm{cm}^{-3}$	$\mu\left/\frac{\mathrm{cm}^2}{\mathrm{Vs}}\right.(77\,\mathrm{K})$	$d/\mu\mathrm{m}$
L 98	5.7	4.4	89488	16
L 111	5.6	2.6	95223	23
L 116	7.2	3.5	81517	20
L 118	10.5	2.3	78069	24

using a *cw* CO_2-laser pumped CH_3F molecular laser of frequency $\omega = 20.2\,\mathrm{cm}^{-1}$ ($\lambda = 496\,\mu\mathrm{m}$) and a HCN-laser of $\omega = 29.7\,\mathrm{cm}^{-1}$ ($\lambda = 337\,\mu\mathrm{m}$). The measurements were performed in Faraday configuration applying the electric bias field perpendicular to the magnetic field.

b) Results

The photoconductive signal of the sample measured at $20.2\,\mathrm{cm}^{-1}$ and $29.7\,\mathrm{cm}^{-1}$ is shown in Fig. 1 as a function of the magnetic field for various biasing conditions. The recordings at $20.2\,\mathrm{cm}^{-1}$ (Fig. 1a) were determined by biasing the sample with a load resistor and a constant voltage source. The measurements at $29.7\,\mathrm{cm}^{-1}$ (Fig. 1b) were performed by applying a constant current source to the sample. The plotted photoconductive signal is the negative of the voltage change as compared to zero irradiation, measured across the sample. Positive or negative photoconductivity implies that the voltage decreases or increases, respectively. At bias fields below the threshold of impact ionization photoconductivity is found to be positive at both laser frequencies in the whole range of the applied magnetic field strength. The narrow lines observed at $B = 1.43\,\mathrm{T}$ with $20.2\,\mathrm{cm}^{-1}$ radiation and at $B = 2.13\,\mathrm{T}$ with $29.7\,\mathrm{cm}^{-1}$ radiation are due to cyclotron resonance of free electrons.

Approaching the impact ionization threshold of the sample by increasing the bias voltage or the current through the sample the photoresponse becomes negative above a certain magnitude of the magnetic field strength. The point where the photosignal crosses the zero line shifts to lower magnetic field with increasing voltage or current, however at $B = 0$ the photoconductivity is always positive. This is demonstrated in Fig. 2 where the photoconductive signal and the voltage across the sample are shown as a function of the current through the sample at zero magnetic field and for $B = 3\,\mathrm{T}$. In both cases the signal increases proportionally to the bias voltages showing the usual behaviour of a photoconductor as far as the operating point is in the high ohmic range

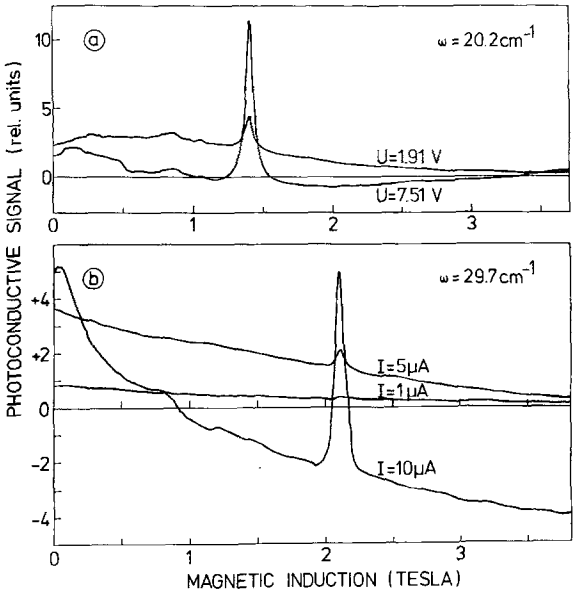

Fig. 1a and b. Photoconductivity at (**a**) $20.2\,\mathrm{cm}^{-1}$ and (**b**) $29.7\,\mathrm{cm}^{-1}$. Measurement (**a**) was performed by a constant voltage source and a load resistor, measurement (**b**) was performed by a constant current source

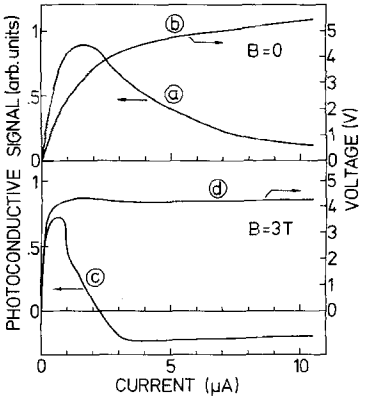

Fig. 2a–d. Photoconductive signal (**a**), (**c**) ($\omega = 29.7\,\mathrm{cm}^{-1}$) and bias voltage (**b**), (**d**) as a function of the current at (**a**, **b**) $B = 0$ and at (**c**, **d**) $B = 3\,\mathrm{T}$. Laser power $\approx 2\,\mathrm{mW}$

of the crystal. Above the impact ionization threshold, where the voltage is almost independent of the current, at zero magnetic field the photoresponse decreases to a very low but always positive level. At a magnetic field of 3 T, for example, however the response crosses zero and becomes negative.

Positive and negative photoconductivity depending on the biasing conditions and the magnetic field can also be observed in a very direct manner by measuring the current voltage characteristic of the epitaxial layer with and without irradiation, as it is displayed in Fig. 3. At $B = 0$ (Fig. 3a) the current of the ir-

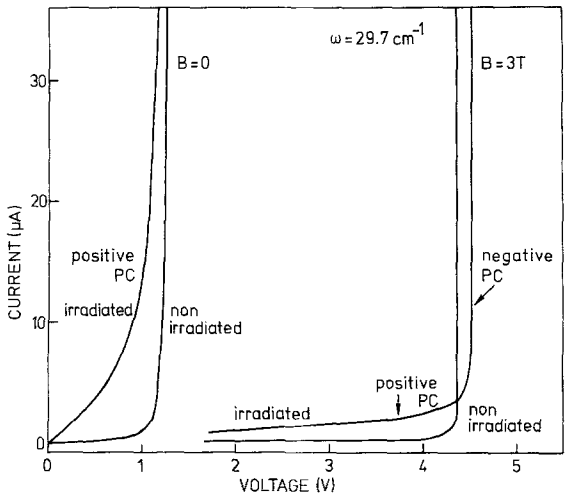

Fig. 3. Current voltage characteristics without and with far-infrared radiation at $B=0$ showing always positive photoconductivity (PC), and at $B=3\,\mathrm{T}$ showing positive and negative PC

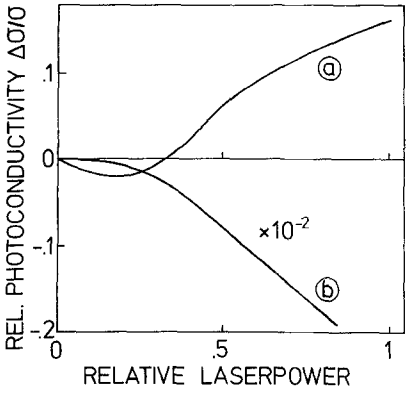

Fig. 4. Photoconductivity at $B=3\,\mathrm{T}$ as a function of the far-infrared laser power ($\omega=29.7\,\mathrm{cm}^{-1}$). The operating point is (**a**) at the threshold of impact ionization (current $I=0.5\,\mu\mathrm{A}$), (**b**) in the infinite slope part of the current-voltage characteristic ($I=50\,\mu\mathrm{A}$)

radiated sample is always larger than the dark current indicating positive photoconductivity. The same result is found at $B=3\,\mathrm{T}$ for biasing voltages below the voltage of impact ionization breakdown, as can be seen from Fig. 3b. The current voltage characteristic of the crystal subjected to irradiation however crosses that of the nonirradiated sample. Thus, irradiation of the sample in a magnetic field increases the threshold voltage of the impact ionization instability and thus causes negative photoconductivity.

Photoconductivity just at the threshold of impact ionization depends nonlinearly on the incident optical power. Figure 4 shows the signal at $B=3\,\mathrm{T}$ as a function of the laser power for two different operating points on the current voltage characteristics. The measurements were performed with an HCN-laser of about 100 mW power at $29.7\,\mathrm{cm}^{-1}$ using calibrated attenuators. At the threshold (Fig. 4a) the signal is negative at low power levels; when the laser intensity is increased negative photoconductivity increases too, attaining a maximum value before decreasing and then becoming positive. In Fig. 4b an analogous measurement is plotted where the operating point was adjusted by a constant current source to be at a very high current in the infinite slope portion of the current voltage curve. In this case the photosignal was found to be negative in the whole available laser power range.

c) Discussion

The shallow donor states in n-GaAs obey to a high accuracy the simple hydrogenic effective mass theory with an effective Rydberg constant R^* of $46.1\,\mathrm{cm}^{-1}$. The magnetic field dependence of donor energy levels was calculated by Larsen [9] and experimentally verified by many investigations [10]. Since the photon energy at $20.2\,\mathrm{cm}^{-1}$ is too small to cause optical transitions between the $1s$ donor ground state and excited states at any magnetic field, positive photoconductivity at this frequency must result from photoionization from excited donor states. At the frequency $29.7\,\mathrm{cm}^{-1}$ $1s-2p_-$ transitions and subsequent thermal or impact ionization of the $2p_-$ state may also contribute to the positive photoconductivity because this frequency falls just in the low frequency wing of the $1s-2p_-$ line and the corresponding transition energy is almost independent of the magnetic field [11].

The experimental results indicate that the presence of a magnetic field and impact ionization of shallow donors as the dominant process of carrier excitation is necessary for the occurrence of negative photoconductivity. If the photoresponse is measured by constant current biasing of the sample, the operating point can be kept in the impact ionization range of the current voltage curve up to high magnetic fields as can be seen from Fig. 3. This is the reason for the persistence of negative photoconductivity with increasing magnetic field strength shown in Fig. 1b. On the other hand, if the sample is biased by a constant voltage source and a load resistor, the operating point moves into the high ohmic range of the characteristic because the threshold voltage of impact ionization increases with magnetic field. Thus negative photoconductivity occurs in a finite range of the magnetic field as observed at $\omega=20.2\,\mathrm{cm}^{-1}$ (Fig. 1a).

III. Theory

a) Generation-Recombination Model

A magnetic field splits the conduction band into Landau subbands and splits and shifts the donor levels in such a way that with increasing magnetic field bound states rise above the bottom of the lowest Landau level. For example the $2p_+$ energy level crosses the low energy edge of the $N=0$ Landau band at a magnetic field strength of about 2T, whereas the $2p_0$ and $2p_-$ levels remain below the lowest conduction band [9]. Higher excited bound donor states submerge at even lower magnetic field strengths into the energy continuum of the conduction band [12]. We assume that negative photoconductivity is due to free to bound optical transitions from the lowest Landau level - populated by impact ionization - to energetically higher donor bound states thus reducing the conductivity of the sample. This assumption explains both requirements found to be necessary for negative photoconductivity: the presence of a magnetic field and impact ionization.

In order to show that these processes give rise to negative photoconductivity and reproduce qualitatively our experimental results we consider a simplified model of an n-type semiconductor with N_D donors, partially compensated by $N_A<N_D$ fully occupied acceptors. We take into account two excited donor states only, one below and one above the low energy edge of the conduction band, representatively, which we call $2p_-$ and $2p_+$. At low temperatures the generation-recombination processes indicated in the level scheme of Fig. 5 are of importance. The generation processes X_1^S and X_2^S are assumed to be induced by the far-infrared radiation neglecting thermal excitations. Impact ionization is considered for the donor ground state and for the first excited state and denoted by X_1 and X_1^*, respectively. This coupled two-step impact ionization process has been shown to produce negative differential conductivity (NDC) and S-type current voltage characteristics, as well as simple impurity breakdown without NDC [6].

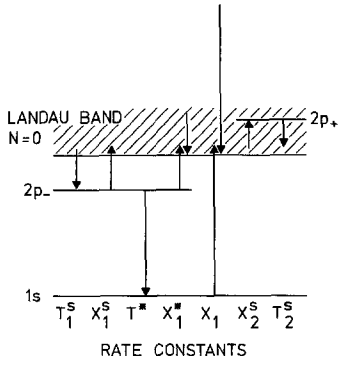

Fig. 5. Schematic energy level diagram and generation-recombination processes taken into account in the model

The rate equations for the generation-recombination processes of Fig. 5 are the following:

$$\dot{n}=X_1^S n_{D^*}+X_1^* n_{D^*} n+X_1 n_D n-T_1^S p_D n-X_2^S n p_D + T_2^S n_1 \tag{1}$$

$$\dot{n}_D=T^* n_{D^*}-X_1 n_D n \tag{2}$$

$$\dot{n}_{D^*}=-X_1^S n_{D^*}+T_1^S p_D n-T^* n_{D^*}-X_1^* n_{D^*} n \tag{3}$$

$$\dot{n}_1=X_2^S n p_D-T_2^S n_1 \tag{4}$$

where n, n_D, n_{D^*}, n_1, and p_D are the concentrations of electrons in the $N=0$ Landau band, $1s$ ground state electrons, $2p_-$ electrons, $2p_+$ electrons, and unoccupied donors, respectively. The rate constants are defined in Fig. 5. From the conservation of the total donor number

$$N_D=n_D+n_{D^*}+n_1+p_D \tag{5}$$

and the charge conservation (local neutrality condition)

$$P_A=n_D+n_{D^*}+n_1+n, \tag{6}$$

where $P_A=N_D-N_A$ is the effective donor concentration, the variables

$$n_{D^*}=P_A-n-n_D-n_1 \tag{7}$$

and

$$p_D=N_A+n \tag{8}$$

can be eliminated in the rate Eqs. (1)-(4).

From (4) one obtains in the steady state

$$n_1=\frac{X_2^S}{T_2^S} n(N_A+n) \tag{9}$$

From (2) and (7) it follows:

$$n_D=\frac{T^*(P_A-n-n_1)}{T^*+X_1 n} \tag{10}$$

$$n_{D^*}=\frac{X_1 n(P_A-n-n_1)}{T^*+X_1 n} \tag{11}$$

Hence the steady state conduction electron concentration is determined by (1):

$$0=(X_1^S+X_1^* n+T^*) X_1 n \left(P_A-n-\frac{X_2^S}{T_2^S} n(N_A+n)\right) - T_1^S(T^*+X_1 n) n(N_A+n) \tag{12}$$

The generation coefficients X_1^S, X_2^S are taken to be proportional to the radiation power P:

$$X_1^S = \alpha P, X_2^S = \gamma P, \frac{X_2^S}{T_2^S} = \eta P \tag{13}$$

Thus (12) can be written as

$$0 = n\{C(n) + B(n)P + A(n)P^2\} \tag{14}$$

where

$$C(n) = T^*(X_1 P_A - T_1^S N_A) + (X_1^* X_1 P_A - (T_1^S N_A + T^*) X_1 - T_1^S T^*) n - (T_1^S + X_1^*) X_1 n^2 \tag{15}$$

determines the dark conductivity $\sigma_d \sim n_d$, where n_d is the concentration of conduction electrons without radiation, and

$$B(n) = \alpha X_1 (P_A - n) - \eta (X_1^* n + T^*) X_1 n (N_A + n) \tag{16}$$

$$A(n) = -\alpha \eta X_1 n (N_A + n) < 0 \tag{17}$$

express the influence of irradiation. For fixed electric biasing field (14) can readily be solved to give

$$P(n) = \{-B \pm \sqrt{B^2 - 4AC}\}/2A$$

and hence $n(P)$ can be computed. This determines the photoconductivity $\sigma(P) \sim n(P)$ as a function of the laser power P, assuming that the dependence of the mobility upon P can be neglected.

b) Photoconductivity

By the following argument it can be decided whether $n(P) > n_d$ (positive photoconductivity) or $n(P) < n_d$ (negative photoconductivity).

Since the impact ionization coefficients X_1, X_1^* depend upon the electric biasing field E, $nC(n) = 0$ by (15) yields the steady state electron concentration under dark conditions as a function of E. Note that $n = 0$ is always a possible, yet not necessarily stable solution. The number and stability of the steady states and the resulting current-voltage characteristics have been discussed in detail elsewhere for the simple kinetics given by (15) and for various elaborations [6]. Depending upon the values of the involved rate constants, two different classes of behavior are obtained: either simple breakdown with a unique stable steady state for all values of the biasing field E (Fig. 6b), or S-shaped negative differential conductivity with bistability between $n = 0$ and $n = n_d$ in some field range (Fig. 6d).

In Fig. 6a, c C is plotted schematically as a function of n for a fixed value of E, larger than the breakdown field, corresponding to monostability (Fig. 6a) and bistability (Fig. 6c). In both cases the following holds:

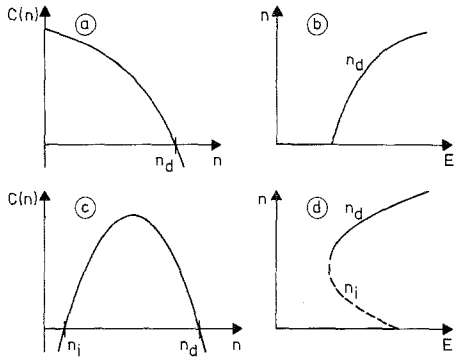

Fig. 6a–d. Schematic plot of the coefficient $C(n)$ in (14) as a function of n for a fixed value of the electric field, and the corresponding electric field dependence $n(E)$ for **(a, b)** one unique stable steady state solution n_d, and for **(c, d)** two steady state solutions n_d and n_i (in addition to $n = 0$), where n_i is unstable

$$\frac{dC}{dn}(n = n_d) \equiv C'(n_d) < 0 \tag{18}$$

For small irradiation power one finds from (14):

$$P(n) \approx -C(n)/B(n) \tag{19}$$

The sign of the photoconductivity is equal to the sign of $P'(n_d) = -C'(n_d)/B(n_d)$. Hence, by (18), the photoconductivity is positive for small P, if $B(n_d) > 0$. On the other hand the photoconductivity is negative for $B(n_d) < 0$, i.e. if the negative term on the right-hand side of (16), which is proportional to the optical pumping rate into the $2p_+$ level, exceeds the term proportional to the photoionization coefficient α of the $2p_-$-electrons. This occurs if the conduction band is highly populated by the impact ionization process. For high optical power $P(n)$ is derived from (14) to be

$$P(n) \approx -B(n)/A(n) \tag{20}$$

and the photoconductivity is always negative ($n < n_d$) because of $n \to 0$ for $A(n) \to 0$.

If stimulated emission from the $2p_+$-level is taken into account, n_1 saturates for large P by (9), and the photoconductivity may become positive again. This can be seen explicitly by setting

$$T_2^S = \tilde{T}_2^S + \tilde{\gamma} P \tag{21}$$

where $\tilde{T}_2^S$ denotes the relaxation constant of the $2p_+$ state by non-radiative processes and spontaneous emission of photons and $\tilde{\gamma}$ is the stimulated emission

coefficient. With

$$\eta=\frac{\gamma}{\tilde{T}_2^S+\tilde{\gamma}P} \tag{22}$$

one obtains from (14) for large P ($\tilde{\gamma}P\gg\tilde{T}_2^S$)

$$P(n)\approx-\tilde{C}(n)/\tilde{B}(n) \tag{23}$$

with

$$\tilde{B}(n)=\alpha X_1\left[(P_A-n)-\frac{\gamma}{\tilde{\gamma}}(N_A+n)n\right]$$

and

$$\tilde{C}(n)=C(n)-\frac{\gamma}{\tilde{\gamma}}(X_1^*n+T^*)X_1n(N_A+n)$$

For

$n_\infty>n_d$, where n_∞ is defined by $\tilde{B}(n_\infty)=0$, i.e. $P(n_\infty)\to\infty$ (24)

this yields positive photoconductivity ($n>n_d$) for large P. For sufficiently large electric fields, however, the inequality (24) cannot be satisfied because, by (15), $n_d\to P_A$, and

$$n_\infty=\frac{1}{2}\left(\frac{\tilde{\gamma}}{\gamma}+N_A\right)\left[\sqrt{1+4P_A\frac{\gamma}{\tilde{\gamma}}\Big/\left(1+\frac{\gamma}{\tilde{\gamma}}N_A\right)^2}-1\right]$$

is independent of the field. This situation is given if the operating point is chosen at a high current in the infinite slope portion of the current voltage characteristic, cf. Fig. 4b.

c) Numerical Results and Discussion

The generation-recombination coefficients introduced in the rate Eqs. (1)–(4) are not known precisely for n-GaAs. Because of the complexity of the rate equations and the large number of unknown parameters it is not reasonable to fit the experimental data by varying the rate constants. Instead we assume arbitrary yet plausible values of the rate coefficients determining the dark conductivity, and present a selection of numerical results for various optical transition constants, whose qualitative behaviour can be compared to the experimental observations.

We consider a half compensated n-type semiconductor, $N_A/P_A=0.5$, and choose for the relaxation constants $T_1^SP_A=10^9\,s^{-1}$ and $T^*=10^6\,s^{-1}$. The impact ionization coefficients are expressed by the Shockley formula [13] with the following numerical parameters:

$$X_1P_A=5\cdot10^8\exp\{(-6\,V/cm/E\}\,s^{-1} \quad \text{and}$$
$$X_1^*P_A=10^9\exp\{(-1.5\,V/cm/E\}\,s^{-1},$$

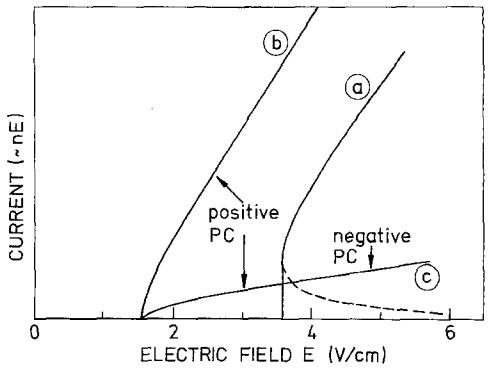

Fig. 7a and b. Calculated current voltage characteristic (**a**) without irradiation (**b**) with photoionization of the $2p_-$ level only ($X_2^S=0$) corresponding to the case $B=0$, and (*c*) including free to bound transitions to the $2p_+$ level corresponding to the experimental situation at $B=3$ T. Rate constants are given in the text

where E is the electric field strength in the semiconductor. These values correspond to typical experimental data for n-GaAs [10, 14].

Now the conduction electron concentration $n(E)$ and thus the current $j\propto n(E)E$ as functions of the electric field can be calculated for appropriate choices of the optical transition constants X_1^S and X_2^S. The results are displayed in Fig. 7. The dark current ($X_2^S=0$, $X_1^S=10^6\,s^{-1}$ by thermal excitation; curve *a*) exhibits a pronounced current controlled negative resistence because both ground state and excited state impact ionization are taken into account [6]. Positive photoconductivity is obtained by assuming a substantial photoionization rate of the $2p_-$ excited donor state ($X_1^S=5\cdot10^7\,s^{-1}$) and neglecting the $2p_+$ state, $X_2^S=0$, (curve *b* of Fig. 7). In this case, corresponding to the experimental situation at zero magnetic field (Fig. 3), the total current exceeds the dark current for all electric fields. If in addition to this, free to bound optical transitions from the conduction band to the $2p_+$-level are taken into account by setting $X_2^SP_A=X_1^S=5\cdot10^7\,s^{-1}$ and $T_2^S=T^*=10^6\,s^{-1}$, positive and negative photoconductivity occurs depending on the strength of the electric field (curve *c* of Fig. 7). This numerical result exhibits the typical experimentally observed behaviour of the current-voltage characteristic of the irradiated sample at $B=3$ T (Fig. 3). Below the impact ionization threshold the current is larger than the dark current; when the electric field is increased above the threshold, the current as a function of E crosses the dark characteristic and remains below the dark current.

Finally the power dependence of the photoconductivity $\Delta n/n_d=(n-n_d)/n_d$ is determined using the same rate constants for the dark current as above. The optical transition coefficients are set $X_1^S=X_2^SP_A=P$,

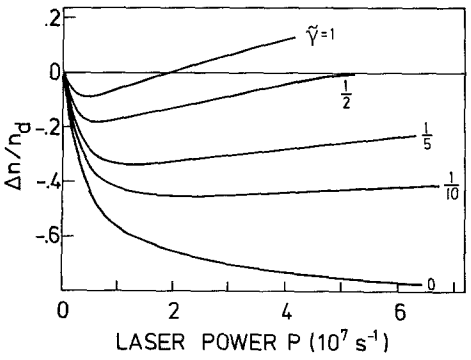

Fig. 8. Relative photoconductivity under impact ionization condition as a function of the optical power P for various stimulated emission coefficients $\tilde{\gamma}$. Rate constants are given in the text

$T_2^S = 10^6\,s^{-1} + \tilde{\gamma}P$ and various stimulated emission coefficients $\tilde{\gamma}$ are taken into account. The calculations are carried out for an electric field strength of 10 V/cm determining an operating point well in the impact ionization range of the current-voltage characteristic of our model system.

The results, displayed in Fig. 8, show that at low optical power levels photoconductivity is in any case negative. At $\tilde{\gamma}=0$ the response is a continuously decreasing function of P; choosing $\tilde{\gamma}>0$ the photoconductivity has a minimum and increases with power. The curve with $\tilde{\gamma}=1$ strongly resembles the corresponding experimental observation shown in Fig. 4a.

IV. Conclusion

Negative far-infrared photoconductivity has been observed in compensated n-GaAs at 4.2 K under experimental conditions which indicate that this effect is due to the change in electron concentration induced by the competition of optical transitions between free and bound electrons and impact ionization. The simplest generation-recombination model incorporating these features has been treated and an explicit condition for negative photoconductivity has been derived: $B(n_d)<0$, cf. (16). The model is tractable analytically and hence allows considerable insight into the mechanism of the negative photoconductivity. Other generation-recombination processes, e.g. excitation of donor electrons from the $1s$ to the $2p_-$ level [6], or relaxation from the $2p_+$ to the $1s$ level, or processes involving other excited levels, could also be taken into account, but this would greatly affect the transparency of the calculations. Such elaborations of more sophisticated models are not expected to change the qualitative features of the model, but only improve the quantitative details.

We are indebted to Dr. E. Bauser, Max-Planck-Institut für Festkörperforschung, Stuttgart, who placed the GaAs samples to our disposal. E. Schöll thanks Prof. F. Schlögl and Prof. N. Klein for encouragement and discussions. W. Heisel and W. Prettl are obliged to W. Böhm and Prof. K.F. Renk for valuable discussions.

References

1. Koenig, S.H.: Phys. Rev. **110**, 986 (1958)
2. Oliver, P.I.: Phys. Rev. **127**, 1045 (1962)
3. Crandall, R.S.: Phys. Rev. B**1**, 730 (1970)
4. Khosla, R.P., Fischer, J.R., Burkey, B.C.: Phys. Rev. B**7**, 2551 (1973)
5. McWhorter, A.L., Rediker, R.H.: Proc. IEEE **47**, 1207 (1959)
6. Schöll, E.: Int. Conf. Hot Carriers in Semiconductors, Montpellier, J. Physique C**3**, 57 (1981)
   Schöll, E.: Z. Phys. B - Condensed Matter **46**, 23 (1982)
7. Crandall, R.S.: Phys. Lett. A**32**, 479 (1970)
8. Heisel, W., Böhm, W., Prettl, W.: Int. J. Infrared Millimeter Waves **2**, 829 (1981)
9. Larsen, D.M.: Phys. Rev. B**8**, 535 (1973)
10. Stillman, G.E., Wolfe, C.M., Dimmock, J.O.: In: Semiconductors and semimetals. Willardson, R.K., Beer, A.C. (eds.) Vol. **12**, p. 169. New York: Academic Press 1977
11. Stillman, G.E., Larsen, D.M., Wolfe, C.M., Brand, R.C.: Solid State Commun. **9**, 2245 (1971)
12. Gershenzon, E.M., Gol'tsman, G.N., Elat'ev, A.I.: Sov. Phys. JETP **45**, 555 (1977)
13. Shockley, W.: Solid State Electron. **2**, 35 (1961)
14. Poehler, T.O.: Phys. Rev. B**4**, 1223 (1971)

E. Schöll
Institut für Theoretische Physik
Rheinisch-Westfälische Technische
Hochschule Aachen
Templergraben 55
D-5100 Aachen
Federal Republic of Germany

W. Heisel
W. Prettl
Institut für Angewandte Physik
Universität Regensburg
Universitätsstrasse 31
D-8400 Regensburg
Federal Republic of Germany